Telechelic Ionomers: Molecular Structure and Kinetics of Physical Gelation of Unsaturated Polyester as Studied by Solid State NMR and X-ray

V. M. Litvinov,* A. W. M. Braam, and A. F. M. J. van der Ploeg

DSM Research, P.O. Box 18, 6160 MD Geleen, The Netherlands

Received August 24, 2000; Revised Manuscript Received November 13, 2000

ABSTRACT: The kinetics of physical gelation and the structure of telechelic ionomers have been studied by ^{1}H and ^{13}C solid-state NMR, SAXS, and WAXD. The reaction of MgO with unsaturated polyesters containing carboxylic and hydroxyl end groups leads to about a 10^3-10^4-fold viscosity increase in the initial solution of polymer in styrene. The results of the present study suggest that the main mechanism, involved in the viscosity increase, is determined by strong electrostatic interactions between Mg^{2+} ions and the charged carboxylato chain ends, resulting in the formation of immobilized ionic multiplets and their aggregates or clusters. Molecular diffusion is the limiting step for cluster formation. SAXS, WAXD, and NMR results suggest a lamella-like structure of the clusters, which are composed of crystalline carboxylato−Mg−aqua complexes in the core part surrounded by a glassy polymer layer with a thickness of a few nanometers. Polyester chains interconnect multiplets, resulting in the formation of a physical network. The estimated distance between neighboring lamella is comparable with the end-to-end distance of network chains. The increase in the content of network chains and immobilized domains causes a large increase in viscosity and storage modulus. The effect of temperature and of ionic and hydroxyl containing additives on the thickening is discussed.

Introduction

Numerous studies have been devoted to gaining an understanding of the molecular structure of polymers with a small content of ion-containing monomer units (up to about 15 mol %).[1] This class of polymers is known as ionomers, as opposed to polymer electrolytes which contain a larger amount of ionic groups. The molecular structure and properties of ionomers have been reviewed by several authors.[1−10] One class of ionomers are telechelic polymers with strongly attracting groups at the chain ends. These polymers are of great interest for both fundamental research and industrial applications because of their unusual mechanical properties. Despite the small content of ionic groups at chain ends, these groups have a strong effect on the properties of these materials. Although the physical structures of ionomers have been studied with a number of techniques, the molecular origin of their properties is still under discussion because of the complexity of the structures formed and the high sensitivity of these structures to the type of ionic functional groups, to counterions, and even to small changes in the composition and chemical structure of the polymer and several other factors. Little is known about the kinetics of the formation of ionomeric structures after ionic bonds are formed during preparation of the ionomers. It appears that this type of information is important for proper understanding of the molecular origin of their properties.

Styrene solutions of unsaturated polyesters (UP) containing carboxylic end groups that are mixed with metal oxides are interesting examples of telechelic ionomers that also find wide industrial application. The reaction of metal oxides with the carboxylic end groups leads to a 10^3-10^4 fold increase in the initial polymer viscosity.[11] This increase in viscosity or thickening reaction is an important parameter in technological materials such as sheet molding compounds (SMC), where the rate of thickening and the resulting viscosity determine the processability of the material. Applications of SMC are found in automotive body panels, appliances, and recreational products. Thickening is usually described in terms of the viscosity regions. In the first region, which occurs during the first few hours after preparation of the compound, viscosity changes are limited. In the second region, the viscosity increases rapidly and the SMC changes from a tacky to a nontacky material. In the third region, the compound does not show a significant change in viscosity and can be molded.

Despite numerous studies, the thickening mechanism of UP is not well understood.[11−14] Three basic mechanisms have been proposed: (1) polymerization mechanism,[15] (2) coordination complex mechanism,[12,16] and (3) ionomeric mechanism.[13,14,17−19] According to all these mechanisms, the thickening starts with an acid−base reaction between a metal oxide (usually MgO) and carboxylic end groups which results in the formation of basic and/or neutral salts. The reaction is accomplished within 2−45 h after addition of MgO to UP. The polymerization mechanism suggests that the viscosity increases mainly as a result of the formation of high molecular weight material by complexing of the carboxylato anions and the metal cations into a neutral salt. The two other mechanisms explain the viscosity increase by the formation of highly branched molecules and/or a physical network. These mechanisms are distinguished by the type of physical junctions that are formed after the acid−base reaction. The coordination complex mechanism suggests that network junctions are formed via the complexing of neutral and/or basic salts by carbonyl oxygen atoms of the ester groups in UP chains and/or hydroxyl end groups. The ionomeric mechanism suggests that the network is formed by

* To whom correspondence should be addressed.

10.1021/ma001478q CCC: $20.00
Published on Web 01/03/2001

Table 1. Composition (in wt %) and Thickening Conditions of Samples Studied

sample	UP0	UP1	UP2	UP3
UP with −COOH and −OH end groups	67	65	65	65
styrene	33 (C_8H_8)	32 (C_8H_8)	32 (C_8D_8)	32 (C_8H_8)
MgO paste in UP with −OH end groups (MgO:UP weight ratio is 1:2)		3	3	3
added water				0.16
thickening temp, °C	30	20, 30	40	30

means of aggregation of magnesium carboxylato salts into ionic clusters, similar to the mechanism in ionomers. Numerous studies of SMC suggest that the ionomeric mechanism is the most realistic one.[13,14,17−20] However, detailed structural information is not available and a possible influence of coordination of other chain portions with Mg^{2+} ions on the viscosity cannot be excluded.

^{1}H and ^{13}C solid state NMR, WAXD, and SAXS experiments were used in this study to determine (1) the structure development during thickening, (2) the molecular structures which are formed during thickening, and (3) the molecular mechanism which is responsible for the viscosity increase. The results are briefly compared with those obtained from a simultaneous study using dynamic mechanical experiments and dielectric spectroscopy.[21] The effects of temperature and water on thickening are discussed.

Experimental Section

A. Samples Studied. The main component of the samples is an unsaturated polyester (UP) dissolved in 33 wt % of styrene. UP was prepared by polycondensation of propylene glycol and maleic anhydride with a slight excess of glycol, followed by dilution in styrene or deuterated styrene. The molar ratio of the anhydride to glycol was about 1:1.01. UP contained both carboxylic and hydroxyl groups at the chain ends (ratio 1:2) and had a typical number-average molar mass of about 1500 g/mol. The polyester was thickened with 3 wt % of a paste of MgO in low molar mass polyester with only hydroxyl groups at both chain ends. The MgO:polyester weight ratio in the paste was 1:2. The composition and thickening conditions of the samples (UP0, UP1, UP2, and UP3) are given in Table 1.

About 0.2 g of each sample was placed in a 9 mm diameter NMR tube of 180 mm length. The upper part of the tube was closed with a poly(tetrafluoro ethylene) stopper in order to prevent evaporation of styrene.

B. Dynamic Viscosity. The rheological characterization was performed on a Bohlin VOR rheometer equipped with a couette of coaxial cylinders geometry. The evaporation of volatiles was minimized with an air lock. The thickening was studied using small amplitude oscillations with an angular frequency of 1 Hz at regular intervals of 10 min in which the sample was left undisturbed. The applied shear strain was kept as low as possible to avoid mechanical breakdown of the developing structure. The temperature was controlled with a thermostat.

C. Solid State NMR Experiments and Data Analysis. 1. Equipment. Proton NMR spin-diffusion experiments, and T_1 and T_2 relaxation experiments were performed on a Bruker Minispec NMS-120 spectrometer. This spectrometer operates at a proton resonance frequency of 20 MHz. The length of the 90° pulse and the dead time were 2.8 μs and 7 μs, respectively. A BVT-3000 temperature controller was used for temperature regulation. The temperature gradient and stability were better than 1 °C.

^{13}C MAS, CP/MAS and inversion−recovery CP/MAS NMR spectra were recorded on a Varian Inova-400 MHz wide-bore NMR spectrometer operating at a ^{13}C frequency of 100.58 MHz, using a 7 mm CP/MAS probe. The ^{1}H and ^{13}C 90° pulse width was about 5 μs.

2. ^{1}H NMR Relaxation Experiments. 2.1. T_2 Relaxation Experiments. Two different pulse sequences were used to record the decay of the transverse magnetization (T_2 decay) from both (semi)rigid and mobile fractions of the samples as described previously.[22] *The solid-echo pulse sequence* (SEPS), $90°_x-t_{se}-90°_y-t_{se}-$[acquisition: A[$f(\tau)$], with $t_{se} = 9$ μs was used to determine the T_2 relaxation time and the proton content of the (semi)rigid fraction of the samples. The time after the first pulse $\tau = 2t_{se}$ was taken as zero. *The Hahn-echo pulse sequence* (HEPS), $90°_x-t_{He}-180°_x-t_{He}-$(acquisition), was used to record the slow decay for the mobile fraction of the samples, where $t_{He} \geq 35$ μs. The second pulse in the HEPS inverts nuclear spins of mobile molecules only and an echo signal is formed with a maximum at time $\tau = 2t_{He}$ after the first pulse. By varying the pulse spacing in the HEPS, the amplitude of the transverse magnetization, $A(2t_{He})$, is measured as a function of time $2t_{He}$. The HEPS makes it possible to eliminate the magnetic field and chemical shift inhomogeneities and to accurately measure the T_2 relaxation time for mobile materials.

The time constants (T_2 relaxation time) that are characteristic of different slopes in the magnetization decay curve, were obtained by performing a least-squares fit of the data using a linear combination of Gaussian and exponential functions for analysis of the T_2 decay, as measured with the SEPS. Only the initial part of the decay ($0 = \tau < 400\mu$s) was fitted. In this fit, the baseline was fixed to the value that was measured at the same conditions after the sample was removed from the NMR probe. A linear combination of two exponential functions was used for analysis of the T_2 decay, as measured with the HEPS. *The relative fraction of the relaxation components,* as designated in the text by % T_2^{index}, represents the fraction of hydrogen in phases/components with different molecular mobility.

The error in the relaxation parameters is composed of (a) experimental errors (about 2%), (b) an error caused by a chosen fitting function (estimated to be about 5%), and (c) uncertainties of the fitting (about 0.5%). Repeated experiments for the same sample indicate that the reproducibility of the results was higher than 2−3%.

2.2. T_1 Relaxation Experiment. The recovery of the longitudinal relaxation was measured with the inversion−recovery pulse sequence using solid echo pulses for the signal detection, $180°_x-t_{var}-90°_x-t_{se}-\ 90°_y-t_{se}-$[acquisition: $A(0)$], with $t_{se} = 9$ μs. Inversion−recovery curves were fitted with a single-exponential function with characteristic time constant T_1. The reproducibility of the results was about 5%.

2.3. Spin-Diffusion Experiment. A modified Goldman-Shen spin-diffusion experiment was performed according to the method described in the literature.[23−25] Solid echo pulses with $t_{se} = 9$ μs were used both in the preparation and the detection phases: $90°_x-t_{se}-90°_y-(t_{se}+t_r)-90°_{-x}-t_m-90°_x-t_{se}-90°_y-$[acquisition: $A[f(\tau)]$. A delay time t_r of 100 μs between the maximum of the first solid-echo and $90°_{-x}$ pulses was used to selectively turn the magnetization of the rigid phase back to the equilibrium. The spin-diffusion experiment was performed twice for each mixing time, t_m, with a 180° phase shift of the first pulse in the second experiment. The free induction decay (FID) from the second experiment was subtracted from the FID obtained in the first experiment. The method largely eliminates the T_1 effect from the recovery of the magnetization due to the spin-diffusion.[24] FIDs recorded at different mixing times were analyzed with a least squares software program developed in our laboratory. The program is not only capable of fitting a single FID but can also be used to obtain a best fit

of an array of FIDs measured at different mixing times (global fit). The global fit adjusts one T_2 value for each relaxation component of FID in the array. It was found by a separate fit of FIDs that T_2 values were not affected by the mixing time within the accuracy of the measurement. The important improvement of the global fit, as compared with a separate fit of each FID, is the high reliability of the "best fit" values of the relative fractions of the relaxation components.

3. ^{13}C NMR Experiments. All experiments were carried out with magic-angle spinning, using a spinning frequency of 3 kHz and high-power proton decoupling. Adamantane was used to optimize the Hartmann−Hahn condition. ^{13}C chemical shifts were referenced to the methylene resonance of adamantane (38.3 ppm relative to tetramethylsilane). ^{13}C CP/MAS spectra were recorded for three different values of the cross-polarization time: 0.08, 0.8, and 8 ms. The cross-polarization time in the inversion−recovery cross-polarization experiment (IRCP) was 0.8 ms. The inversion time in the IRCP was varied from 0.05 to 8 ms. The pulse sequences used are described elsewhere.[26]

D. Calculation of the Mean Molar Mass between Physical Junctions. The distinguishing feature of T_2 relaxation for viscoelastic networks is the high-temperature plateau that is observed at temperatures well above T_g. The temperature independence of T_2 is attributed to constraints, which limit the number of possible conformations of a network chain with respect to those of a free chain. The theory of the transverse relaxation in elastomeric networks relates T_2 at the high-temperature plateau to the number of statistical segments, Z, between chemical and physical network junctions[27−29]

$$Z = (T_2^{pl})/[a(T_2^{rl})] \quad (1)$$

where a is the theoretical coefficient, which depends on the angle between the segment axis and the internuclear vector for the nearest nuclear spins at the main chains. For polymers containing aliphatic protons in the main chain, the coefficient a is close to 6.2 ± 0.7.[28] T_2^{rl} is the relaxation time that was measured below T_g for polymer swollen in a deuterated solvent. T_2^{rl} for UP is 0.0154 ± 0.0003 ms. Using the number of backbone bonds in the statistical segment, C_∞, the molar mass of network chains, M_w, is calculated

$$M_w = ZC_\infty M_u/n \quad (2)$$

where M_u is the average molar mass per elementary chain unit for the copolymer chain and n is the number of backbone bonds in an elementary unit. C_∞ of about 4−5 rotatable bonds of the UP backbone was used for the calculation.

E. NMR Study of Molecular Heterogeneity. 1. Molecular Mobility and the Content of Phase/Components. The sensitivity of the T_2 relaxation to the molecular scale heterogeneity is due to the local origin of the relaxation process, which is predominantly governed by the nearest-neighbor environment and intramolecular effects for T_2 relaxation. The analysis of the T_2 decay is often used for the determination of phase composition and molecular heterogeneity in polymers. In a simplified picture, the total T_2 relaxation decay for a heterogeneous polymer is a weighted sum of decays from different phases, components or polymer chains/submolecules, such as network chains, free chains, and chain-end blocks.[22,30] If the molecular mobility of these species differs significantly, the transverse relaxation reveals distinct components. *The relative fraction* of these components is proportional to the hydrogen content in these species. The analysis of T_2 decays often makes it possible to obtain accurate, quantitative data on the composition as well as characteristics of molecular motion in different phases.[30] It should be mentioned that the multicomponent relaxation does not always indicate microphase separation. For example, the rotational mobility of small molecules, which are homogeneously dispersed in the polymer matrix, could significantly differ from the mobility of polymer chains. Multicomponent relaxation could also be caused by several other factors such as (a) the complex origin of molecular motion in the case of long chain molecules, (b) wide or bimodal distribution of the correlation time of molecular motions, and (c) spatial heterogeneity of chain motion which is caused by morphological heterogeneity of the sample on a scale of at least a few nanometers.

2. Estimation of Domain Size. The spin diffusion experiment is used for estimating of the size of immobilized domains.[23−25] The recovery of the longitudinal magnetization of rigid material, $M_r(t_m)/M_r^{eq}$, in the spin-diffusion experiment is determined by the size and shape of immobilized domains surrounded by soft matrix, and by the spin-diffusion coefficient D_{eff}. Values of $M_r(t_m)$ and M_r^{eq} represent the relative value of the transverse magnetization for rigid material at mixing time t_m in the spin-diffusion experiment and its equilibrium value, respectively. The size of immobilized domains, d_{im}, can be estimated from the initial slope of the dependence $M_r(t_m)/M_r^{eq}$ on $(t_m)^{0.5}$ using the following equation[23−25,31−35]

$$d_{im} = k[4D_{eff}(t^s{}_m)/\pi]^{0.5} \quad (3)$$

where $(t^s{}_m)^{0.5}$ is the time at which the extrapolated straight line that describes the initial slope of a spin-diffusion curve reaches the value of $M_r(t_m)/M_r^{eq} = 1$; the dimensionality constant k is 1 for a lamellar system, 2 for a cylindrical geometry, and 3 for spherical phases; D_{eff} is the effective spin diffusion coefficient.[31,32] It is mentioned that the spin-diffusion coefficient cannot be determined accurately for disordered polymers with complex chemical structures and materials those morphology is not well-defined. A typical value of D_{eff} of about 0.7 nm^2/ms is used for the estimation of the domain size.[34] The estimated domain size suffers from a large error because the derivation of eq 3 is based on several assumptions[35] and because the value of D_{eff} is an approximate one.

F. X-ray diffraction experiments. 1. WAXD. Wide-angle X-ray diffraction experiments were performed with a powder diffractometer PW1820 using Cu Kα-radiation (40 kV, 50 mA) and fixed slits. The radiation was monochromatized with a monochromator in the diffraction beam. Silicon single crystals were used as sample holders. Samples were spinned to avoid the samples to flow out of the sample holders. Air scattering was suppressed using helium as a purge gas.

2. SAXS. Small-angle X-ray scattering experiments were performed using a Kratky camera with a 30 μm slit using Cu Kα radiation (40 kV, 50 mA). The radiation was monochromatized with a Ni-filter in the primary beam and an energy discriminator at the detector. A Braun OED-50M linear position sensitive detector was used with a sample-to-detector distance of 388 mm. Low viscosity samples were measured in X-ray capillaries of 1 mm diameter; high viscosity samples were mounted on a tape.

3. SAXS Data Treatment. Data treatment was performed with FFSAXS.[36] Scattered intensities were corrected for instrumental effects by subtracting intensities originating from identical experiments without samples (i.e., capillary or mounting tape). Liquid scattering was subtracted assuming a constant intensity level. Desmeared intensities, I, were obtained according to the infinite-slit-approach.[37] Intensities, $I(s)$, are presented as a function of the scattering vector s, $s = 2(\sin\theta)/\lambda$, with 2θ being the angle between the incident and scattered beam and λ being the wavelength. For the lamellar type systems, it is more useful to interpret it 1-dimensionally; intensities, $I_1(s)$: $I_1(s) = l(s)\, s^2$. In the absence of interference effects, particle/domain sizes can be obtained, as described in for instance reference.[38] For lamellar particles the radius of gyration, R_t, follows from

$$l_1(s) = l_1(0) \exp(-4\pi^2 s^2 R_t^2) \quad (4)$$

An alternative route to determine particle sizes is by means of correlation functions. In this way the influence of interference effects is reduced according to the procedure described above. A one-dimensional correlation function, $\gamma_1(r)$, was calculated from smeared intensities.[39] The minimum value of the one-dimensional correlation function, γ_{min}, provides an

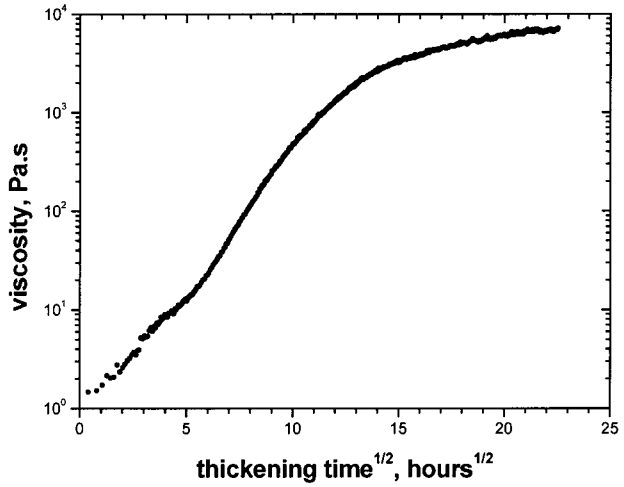

Figure 1. Viscosity of UP1 as a function of the square root of the thickening time. Thickening was performed at 30 °C.

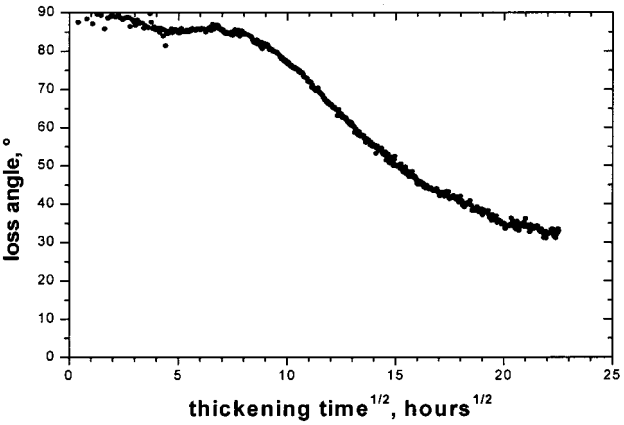

Figure 2. Loss angle of UP1 as a function of the square root of the thickening time. Thickening was performed at 30 °C.

estimate of the volume fraction of the phase that is present in minor concentration. If we describe $\gamma_1(r)$ at $r \rightarrow 0$ as a straight line, the intercept of this line with $\gamma_1(r) = \gamma_{min}$ indicates the size of the phase present in minor concentration.

Results

1. Viscosity as a Function of Thickening Time. The thickening of UP1 at 30 °C is plotted in Figures 1 and 2 for the dynamic viscosity and loss angle, respectively. The loss angle δ is a measure of the elasticity of the system where $\delta = 0°$ represents an elastic and $\delta = 90°$ a fully viscous material. The viscosity and the loss angle show a tremendous change as a function of the thickening time. The molecular origin of these phenomena will be discussed below.

2. Structural Heterogeneity As Studied by ^{1}H T_2 Relaxations. 2.1. Formation of Heterogeneous Structures During Thickening. The decay of the transverse magnetization for UP0 is shown in Figure 3. The T_2 decay consists of two components with characteristic decay times of 2.3 and 29 ms. The relative fraction of these components is 16% and 84%, respectively. The strong deviation from a single-exponential relaxation for UP0 suggests a wide distribution in the molecular mobility.[40]

A third relaxation component was detected for UP1 shortly after it was mixed with MgO (see Figure 4). These relaxation components are designated by superscripts "s", "in" and "l" which correspond to short (T_2^s),

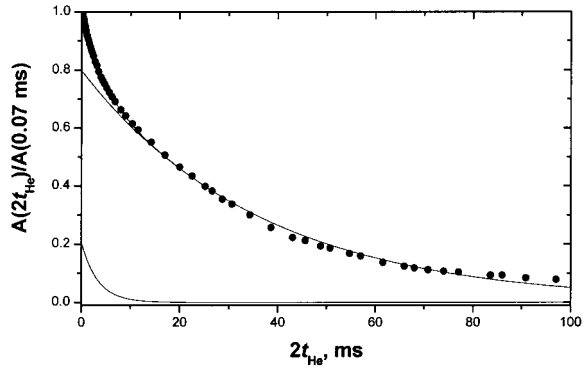

Figure 3. Decay of the transverse magnetization (points) at 30 °C for UP0. The decay was measured with the HEPS. Solid lines represent the result of a least-squares adjustment of the decay with a linear combination of two exponential functions and the separate components.

intermediate (T_2^{in}) and long (T_2^l) decay times, respectively. Values of % T_2^s, % T_2^{in} and % T_2^l represent the relative fraction of these components. Both the relaxation times and the relative fractions change with thickening time (see Figures 5 and 6). The relative fraction of T_2^s increases with thickening time, as can be seen from Figures 4 and 6. This relaxation component is characterized by a short T_2 that is typical of polymers in the proximity of T_g. It is mentioned that the fast-decaying component could not originate from a magnetic susceptibility effect in heterogeneous material, especially if the experiment is performed with low field NMR equipment, as in our case.[22] Since MgO is dissolved during the first few hours after preparation of the compound, it can be suggested that *the T_2^s relaxation component originates from polyester chain units that are immobilized due to interactions with Mg^{2+} ions*. An additional proof of this assignment is provided by NMR spin-diffusion experiments, WAXD and SAXS. According to these experiments, the results of which will be discussed below, immobilized domains are formed during thickening.

The assignment of the two other T_2 relaxation components is less rigorous. A quantitative analysis of the decay shape for polymer chains above T_g is not always straightforward due to the complex origin of the relaxation itself[47] and the apparent heterogeneity of the samples studied.[40] Moreover, the interpretation of the relaxation data is complicated due to the presence of styrene monomer, whose contribution to the total magnetization in UP1 is about 50%. To find out the molecular origin of T_2^{in} and T_2^l relaxation, the following experiments were performed: (1) thickening was studied for UP2 containing deuterated styrene, and (2) the temperature dependence of T_2 relaxation was studied for thickened UP1.

The ^{1}H T_2 relaxation for UP2 *is entirely determined by the relaxation of the polyester chain*. The T_2 decay of UP2 is also composed of three components with about the same values of T_2^s, T_2^{in} and T_2^l (see Figure 7). The dependence of the relaxation parameters against thickening time is rather similar for UP1 and UP2. In both cases the fraction of the relaxation components % T_2^s and % T_2^{in} increases at the expense of % T_2^l (see Figures 6 and 8), and the relaxation times T_2^s, T_2^{in}, and T_2^l decrease with thickening time, (see Figures 5 and 7). These changes in relaxation parameters are apparently related to an overall decrease in molecular mobility during thickening, because shorter T_2 values for oligo-

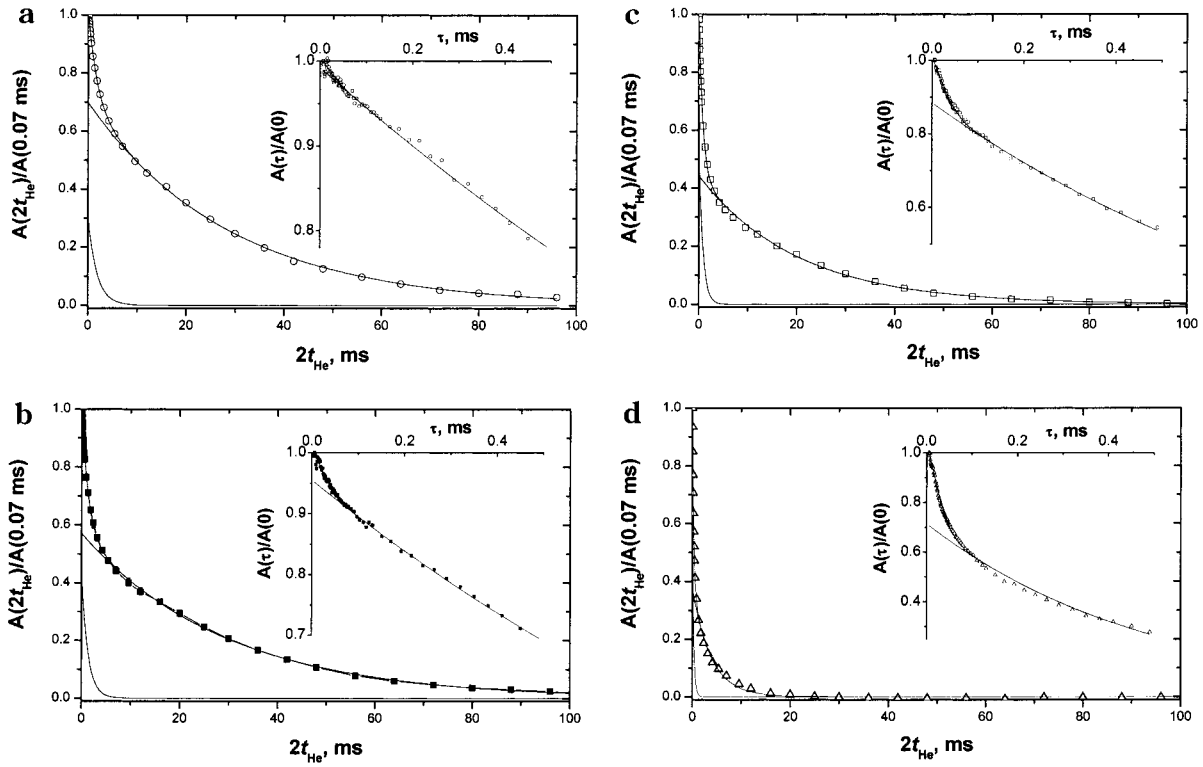

Figure 4. Decay of the transverse magnetization (points) at 30 °C for UP1 at different times after the compound was prepared: (a) 22 h; (b) 103 h ; (c) 506 h; (d) 2524 h. Thickening was performed at 30 °C. The decay was measured with the HEPS. Solid lines represent the result of a least-squares adjustment of the decay with a linear combination of two exponential functions and the separate components. The initial part of the decay, as measured with the SEPS, is shown on the insert on the right-hand side of the plots.

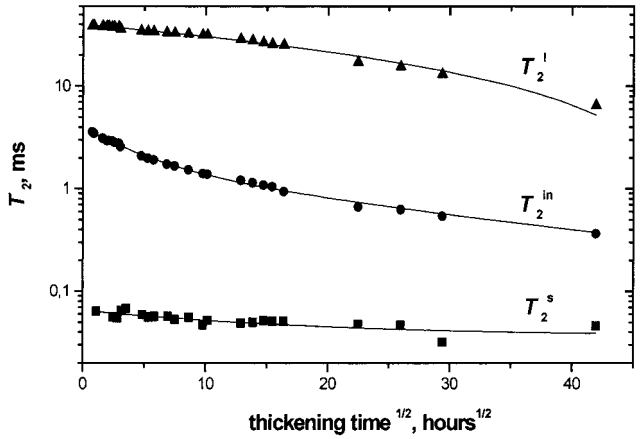

Figure 5. T_2 relaxation times for UP1 as a function of the square root of the thickening time. Thickening was performed at 30 °C. The lines shown are a guide to the eye.

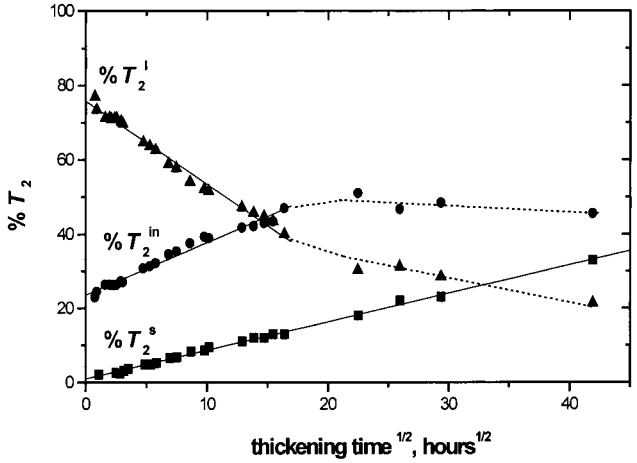

Figure 6. Relative fraction of the relaxation components for UP1 as a function of the square root of the thickening time. The dotted lines are a guide to the eye. Solid lines represent the results of a linear regression analysis of the data for thickening time up to 240 h: % T_2^s [intercept = 0.98 ± 0.15%; slope = 0.77 ± 0.01%/$h^{1/2}$; the correlation coefficient equals 0.998]; % T_2^{in} [intercept = 23.6 ± 0.4%; slope = 1.42 ± 0.05%/$h^{1/2}$; the correlation coefficient equals 0.990]; % T_2^l [intercept = 75.7 ± 0.5%; slope = −2.22 ± 0.07%/$h^{1/2}$; the correlation coefficient equals 0.993]. Thickening was performed at 30 °C.

mer molecules above T_g correspond to more hindered long spatial scale chain mobility.[41−47] The results for UP2 provide considerable evidence that the origin of the relaxation components is largely determined by heterogeneity in the molecular mobility of UP chains and that the mobility of styrene molecules is strongly coupled to that of UP chains. Since the fraction of the relaxation components changes significantly with thickening time after the acid−base reaction between MgO and carboxylic end groups is fully accomplished, this suggests that these changes are *caused by physical interactions between polyester chains and* Mg^{2+} *ions.*

2.2. The Effect of Temperature on Structural Heterogeneity. Analysis of the temperature dependence of the T_2 relaxation can provide information on the origin of physical interactions, since the mobility of polymer chains is largely determined by physical structures and morphology, as well as their dependence on temperature.[30,31,47] The temperature dependence of T_2 relaxation parameters for thickened UP1 is shown in Figures 9 and 10. T_2^s hardly changes with temperature. This means that chain mobility in the immobilized domains is strongly hindered up to 120 °C, the highest

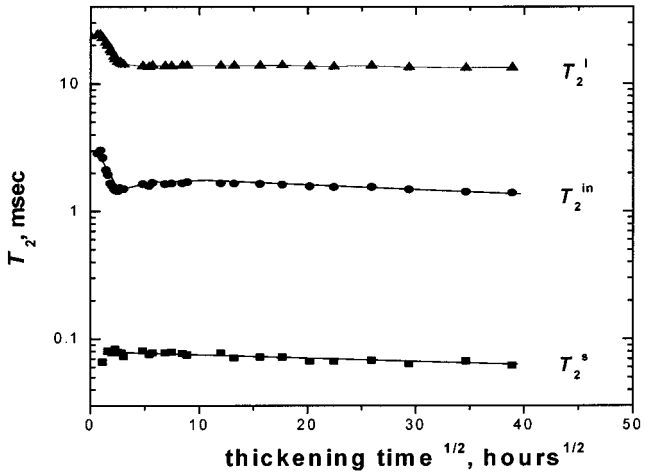

Figure 7. T_2 relaxation times for UP2 as a function of the square root of the thickening time. Thickening was performed at 40 °C. The lines shown are a guide to the eye.

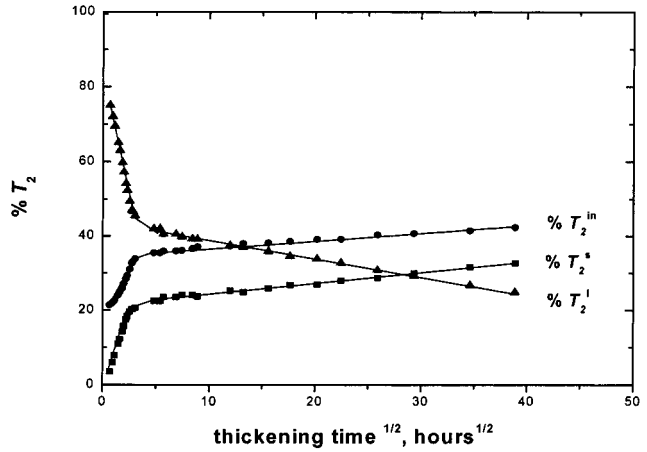

Figure 8. Relative fraction of the relaxation components for UP2 as a function of the square root of the thickening time. The lines shown are a guide to the eye. Thickening was performed at 40 °C.

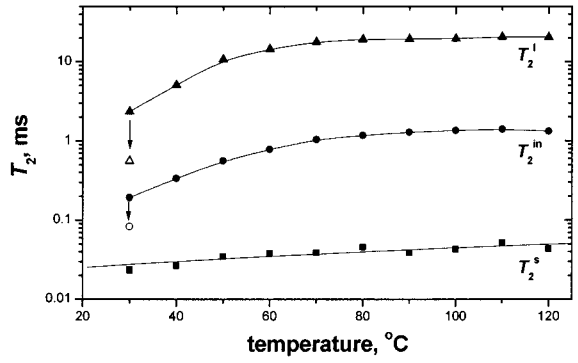

Figure 9. T_2 relaxation times as a function of temperature for UP1 after the compound was stored at 30 °C for 160 days. The dependence was measured at stepwise heating of the sample from 30 to 120 °C. Open points show the relaxation times that were measured shortly after the sample was cooled from 120 to 30 °C. The lines shown are a guide to the eye.

temperature at which the experiments were performed. The fraction of these domains decreases with increasing temperature. Cooling down of the sample results in immediate recovery of the structures that were formed during prolonged thickening before the sample was heated. The change in the content of immobilized domains upon heating and subsequent cooling proves

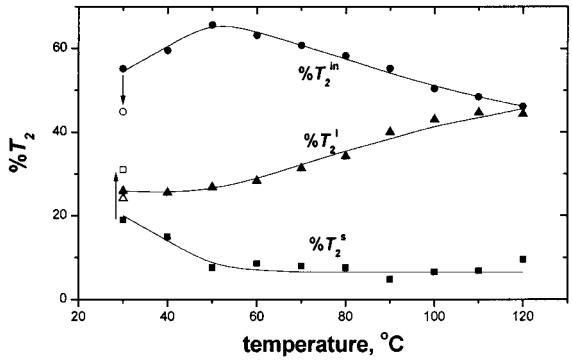

Figure 10. Relative fraction of the relaxation components as a function of temperature for UP1 after the compound was stored at 30 °C for 160 days. The dependence was measured at stepwise heating of the sample from 30 to 120 °C. Open points show the fraction of the relaxation components that were measured shortly after the sample was cooled from 120 to 30 °C. The lines shown are a guide to the eye.

the physical origin of the interactions that are responsible for the formation of the immobilized domains.

Above 80 °C, T_2^{in} is close to 1 ms, and it does not increase significantly when the temperature is increased further (see Figure 9). Such a high-temperature plateau of the T_2 relaxation is observed for vulcanizates at temperatures well above T_g.[27−29] It should be mentioned in this connection that T_2^{in} is in the range which is typical of viscoelastic chains in vulcanizates and physical networks.[22,29,30,47,48] The relaxation time T_2^{in} at the high-temperature plateau, $(T_2^{in})^{pl}$, can be used for determining the mean molar mass of network chains which are formed by chemical and physical junctions.[27−29,48,49] The mean molar mass of network chains in UP1 is estimated from eqs 1 and 2. Its value equals about 1000−1500 g/mol at temperatures above 80 °C. This value is comparable with the mean molar mass of polyester chains. It is therefore concluded that polyester chains are anchored to immobilized domains at chain ends and form bridges between neighboring immobilized domains.

On the basis of the above results, *the relaxation component T_2^{in} is presumably to be attributed to the relaxation of network chains ("chain bridges") that are formed by chain anchoring to immobilized domains or clusters.* The third relaxation component has a long decay time T_2^l that is comparable to that for initial UP0. *This component is presumably to be attributed to styrene molecules and polyester chains that are not attached to immobilized domains, as well as to highly mobile network defects such as dangling chains and chain loops.* It should be mentioned that the assignment of the T_2^{in} and T_2^l relaxation is highly simplified, as it was discussed for UP0,[40] and *values of T_2^{in}, T_2^l, % T_2^{in}* and *% T_2^l should be considered as relative characteristics of the effect of thickening time on the T_2 relaxation rather than absolute characteristics of structures which are formed during thickening.*

3. Chemical Origin of Heterogeneous Structures As Studied by ^{13}C NMR Spectroscopy. It appears that immobilized domains play an important role in the thickening of UP. To obtain information about the chemical composition of these immobilized domains and of the soft matrix the following ^{13}C solid-state NMR spectra were recorded: MAS spectra, CP/MAS spectra at short, intermediate, and long cross-polarization times, and IRCP spectra at different inversion times.

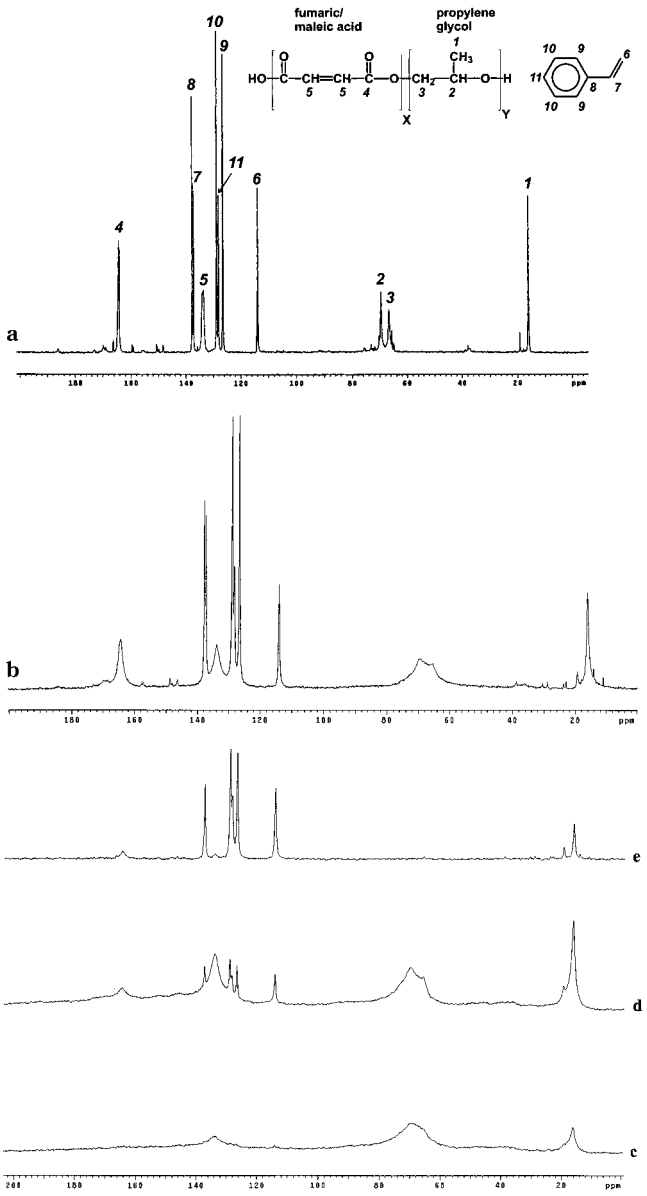

Figure 11. ^{13}C MAS spectra for initial UP0 (a) and thickened UP1 (b) and ^{13}C CP/MAS spectra for thickened UP1 at cross-polarization times of 0.08 ms (c), 0.8 ms (d), and 8 ms (e). Spectra b−e were recorded 45−50 days after the compound was made. The compound was stored at 30 °C before the experiments were performed. According to the proton relaxation experiment, the thickened UP1 contains about 12 at. % hydrogen in immobilized domains. The spectra were recorded at room temperature. The assignment of resonances with the largest integral intensity to different types of carbon atoms is shown in part a. Small peaks correspond to resonances of end groups, additives, and etherification products.

It is noted that neither ^{1}H nor ^{13}C NMR data provide any information about the partitioning of Mg^{2+} ions between immobilized and soft materials.

^{13}C MAS spectra were recorded for initial UP0 and thickened UP1. The ^{13}C MAS spectrum for initial UP0 shows well resolved resonances that correspond to different types of carbon atoms, as indicated in Figure 11a. All resonances of polyester carbons for UP1 (see Figure 11b) are significantly broader than those of UP0. The line broadening is caused by a restriction of chain mobility.

The ^{13}C resonances of highly immobilized phases/components in heterogeneous materials are enhanced in ^{13}C CP/MAS spectra at short cross-polarization time (τ_{cp}) and diminish at very long τ_{cp}. By contrast, the resonances from mobile phases/components are enhanced at long τ_{cp} and are hardly detected at very short τ_{cp}. It should be mentioned that the line intensity as a function of τ_{cp} in ^{13}C CP/MAS spectra is also affected by the chemical origin of carbon atoms. It can be seen from Figure 11c−e that only broad resonances from polyester chains are present in the spectrum at short τ_{cp}. Resonances from styrene molecules are mainly observed at long τ_{cp}.

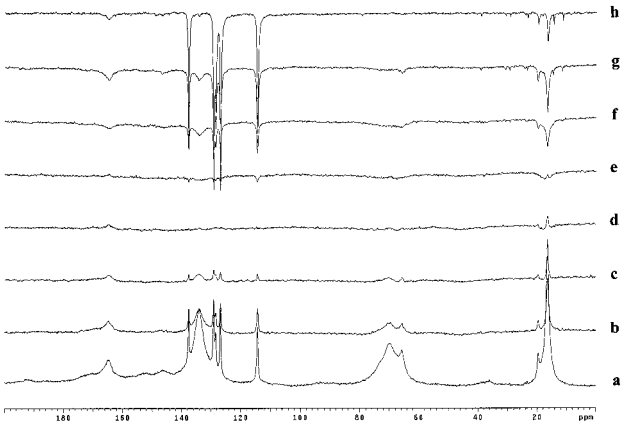

Figure 12. ^{13}C inversion−recovery CP/MAS spectra for the thickened UP1. The spectra were recorded 55 days after the compound was made. The compound was stored at 30 °C before the experiments were performed. The cross-polarization time is 0.8 ms. The inversion times are 0.05 (a), 0.4 (b), 0.65 (c), 0.8 (d), 0.95 (e), 1.5 (f), 3 (g), and 8 ms (h). The spectra were recorded at room temperature.

The ^{13}C inversion−recovery CP/MAS spectra reveal that all resonances of polyester carbons are inverted at about the same inversion time. The crossover time was observed to be about 0.9 ms. (Figure 12d,e). This means that the mobility of *all backbone carbons* is suppressed in well-thickened UP1 to about the same extent.

Thus, ^{13}C NMR data show that the immobilized domains are enriched in polymer content compared to the bulk composition. Since the mobility of the chain units of different chemical structures is hindered to about the same extent, it might also be suggested that there are several reasons for immobilization of organic material in the domains: i.e., ionic interactions between carboxylato chain ends and Mg^{2+} ions, coordination bonds of Mg^{2+} with hydroxyl chain ends, carbonyl and ester groups in middle portions of polyester chains, and topological constraints and steric hindrances.

4. Domain Size As Determined by NMR. According to the present results, the immobilized domains play an important role in the thickening of UP. Spin-diffusion and spin−lattice (T_1) relaxation experiments were used to estimate the shortest distance across the immobilized domains. The T_1 relaxation can be described fairly well by a single exponent. This suggests that spin-diffusion is very efficient in the sample. The maximum distance over which spin diffusion is effective at the time scale of the T_1 relaxation is on the order of 50 nm.[23] Thus, the size of the immobilized domains should be of the same order or less. The primary data of the spin diffusion experiment are shown in Figure 13. The T_2^s relaxation component vanishes at short mixing times in the spin-diffusion experiment and gradually recovers to its equilibrium value with increasing mixing time, which proves the existence of immobilized domains.[23]

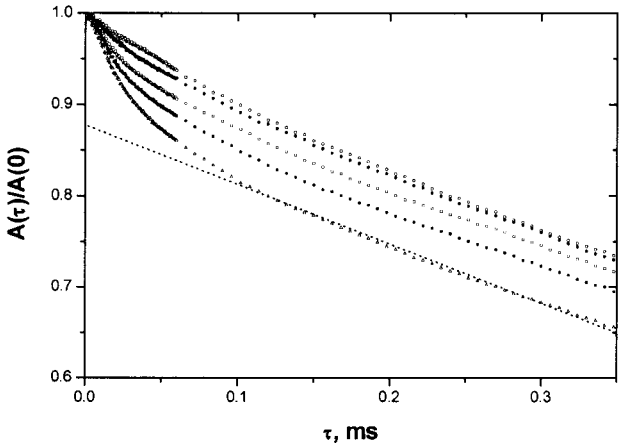

Figure 13. Free induction decay (FID) in the spin diffusion experiment at different mixing times for UP1 after thickening at 30 °C for 652 h. The FID at mixing times of 0.1, 0.2, 2, 8, and 100 ms is shown by open and closed circles, open and closed squares, and triangles, respectively.

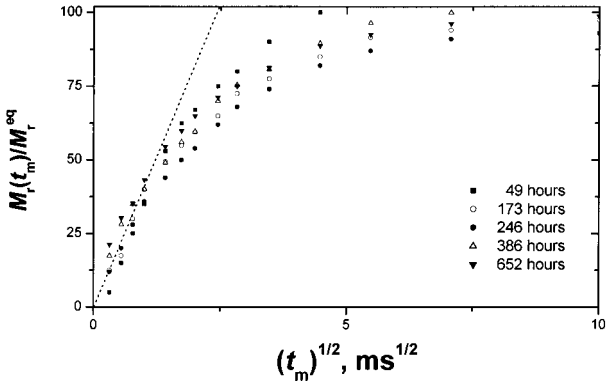

Figure 14. Results of the spin diffusion experiment for UP1 which show the recovery of magnetization for immobilized domains, $M_r(t_m)/M_r^{eq}$, with increasing mixing time in the experiment, where $M_r(t_m)$ and M_r^{eq} are the fractional amplitudes of the transverse magnetization of the immobilized domains at mixing time t_m and at equilibrium, respectively. The different symbols correspond to different storage times (in hours) of the compound at 30 °C, as shown in the figure. The dotted line shows the initial slope of the spin-diffusion curve.

The recovery of the magnetization from immobilized domains, $M_r(t_m)/M_r^{eq}$, is shown in Figure 14. With $(t^s_m)^{0.5} = 2.5$ ms$^{0.5}$ (see eq 3), the shortest distance across the immobilized domains equals about 6, 12, or 18 nm for a hypothetical lamellar, cylindrical, or spherical geometry of these domains in UP, respectively. The estimated distance should be considered as a very approximate value, as discussed in the experimental part. The initial slope of the spin-diffusion curve is hardly affected by thickening, which means that *the shortest distance across immobilized domains does not change significantly upon thickening.*

5. Heterogeneity As Studied by X-ray Diffraction. The nature of the domains is studied by WAXD. UP1 appears to be completely amorphous immediately after preparation. The experiment, which was performed 110 days after the compounding, revealed a crystalline phase, as can be seen from Figure 15. Although the signal of this phase is weak, it clearly demonstrates its crystalline nature. Apparently, the crystalline phase originates from the immobilized domains. The Bragg reflections of the crystalline phase do not originate from a 1-dimensional lattice. The

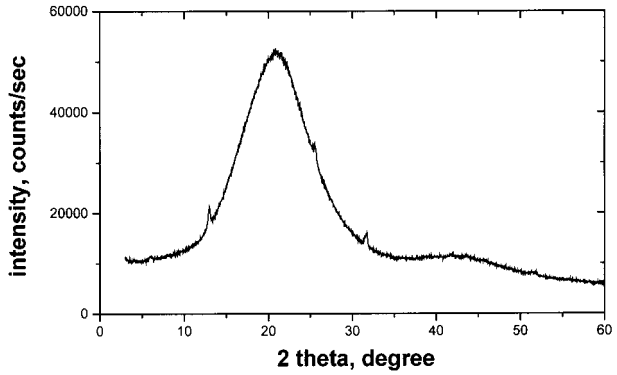

Figure 15. WAXD pattern of UP1 recorded 110 days after the compound was made. Thickening was performed at 30 °C.

crystal lattice is at least 2-dimensional. WAXD data excludes spherical and cylindrical shape of immobilized domains. This shape of the domains will not cause sharp crystalline reflections because of small domain sizes in at least one dimension, which follows from the spin-diffusion experiment. Thus, *a lamella-like shape of the domains is the most likely*.

Small-angle X-ray scattering data can provide information about the heterogeneous structures in UP1. Figure 16a presents $I_1(s)$ for UP1 shortly and 110 days after compounding. Fresh UP1 shows a continuous decrease in intensity with increasing s, indicating that the sample contains a small amount of the domains, randomly distributed. After 110 days of thickening, $I_1(s)$ shows a broad intensity maximum, indicating a substantial increase in heterogeneity that is in agreement with NMR data. The immobilized domains can be considered to form a superlattice. The lattice distances vary from 2 to 12 nm with a preferred lamellar spacing of 3 nm, as can be seen from the results in Figure 16a.

Additional information about the lattice distances is obtained from the one-dimensional correlation function, $\gamma_1(r)$. The features of the correlation function are first discussed for UP1 thickened for 110 days (see Figure 16c). Positive values of $\gamma_1(r)$ are observed at $r > 2.5$ nm. This confirms the result that the lamellar domains are stacked on a superlattice with spacings larger than 2.5 nm. Since a clear maximum in $\gamma_1(r)$ is lacking, this implies that the superlattice is very irregular. In other words, the lamellae are not stacked well. Furthermore, $\gamma_1(r)$ reaches a minimum at $\gamma_{min} = -0.4$. This implies that the volume fraction of the immobilized domains is at least 30%. This value is in good agreement with the content of immobilized domains, as measured by NMR for the same sample with similar thickening time (see Figure 6). Via extrapolation of the linear part of the decline of $\gamma_1(r)$ (at $r > 0$) to γ_{min}, a lamellar thickness of about 1 nm is estimated.

The value of $\gamma_1(r)$ does not reach a negative value for UP1 analyzed shortly after compounding. This confirms the absence of a superlattice in the fresh sample. Nevertheless, it has to be mentioned that even in this case a small minimum in $\gamma_1(r)$ occurs at the same r, where thickened UP1 shows a distinct minimum. This indicates that even shortly after compounding UP1 contains some heterogeneity, which causes interference effects. The superlattice seems to be already present, but it is not yet fully developed.

The radii of gyration of the lamella can be calculated from the results in Figure 16b, if interference effects are ignored. This figure shows a straight line in a large

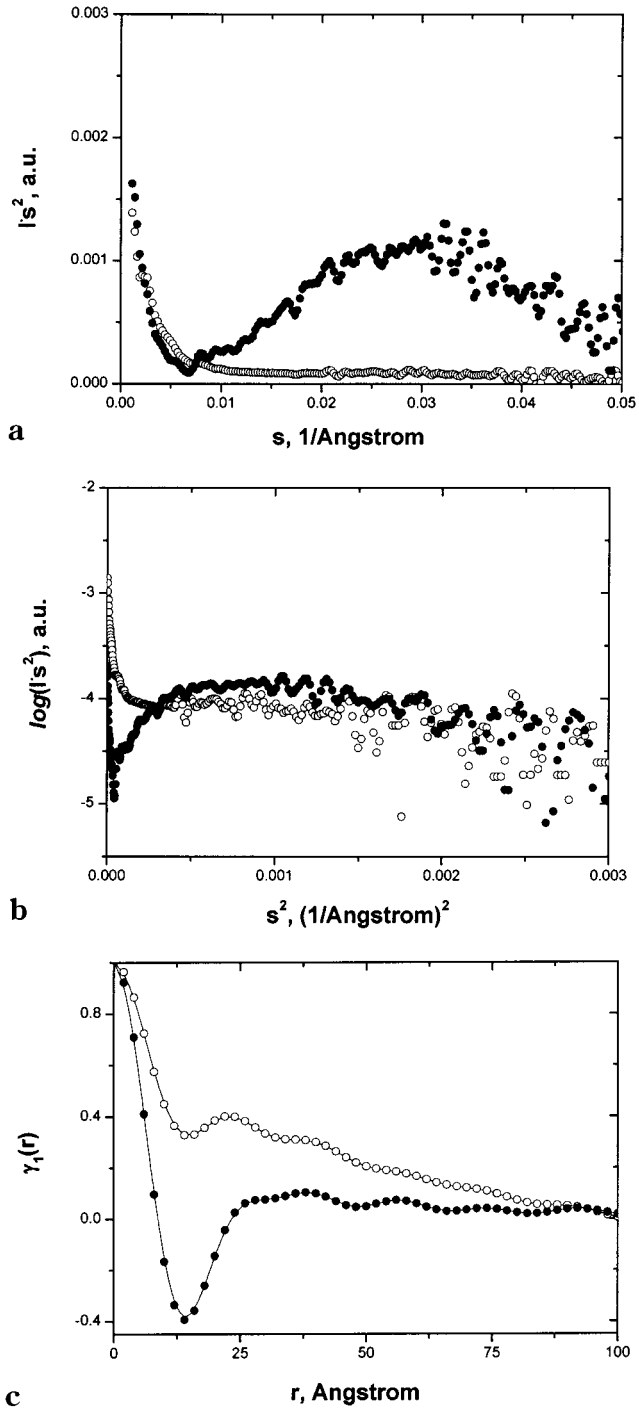

Figure 16. SAXS data for UP1 recorded shortly after the compound was made (open circles) and after 110 days of thickening at 30 °C (closed circles): (a) desmeared one-dimensional intensities $I_1(s)$; (b) $\log[I_1(s)]$ as a function of s^2; (c) the correlation function $\gamma_1(r)$.

range of s^2 for freshly made UP1. The radius of gyration, R_t, of 0.25 nm is calculated from the slope of this line. This value corresponds to the lamellar thickness of 0.9 nm, assuming that the lamellae have the same thickness and uniform density. Interference effects introduce a strong deviation from the straight line for thickened UP1, as is clearly seen in Figure 16b. Nevertheless, a straight line is also found at smaller range of s^2 indicating that the lamellar thickness is hardly affected by thickening time, which is in agreement with the results of the spin-diffusion experiments. The lamellar thickness of 0.9 nm is estimated for thickened UP1. This value is very close to that obtained from $\gamma_1(r)$, i.e., 1 nm.

Thus, NMR and X-ray data show that *lamella-like immobilized domains are formed shortly after mixing of UP with MgO and the lamellae grow in lateral direction*. The nature of these domains will be defined in the Discussion.

Discussion

The Molecular Mechanisms of Thickening. WAXD shows that crystalline lamella-like domains are formed during thickening of UP. According to NMR, a thin layer of immobilized polyester chain units surrounds these domains. Immobilized domains have been detected by various techniques in ionomers.[1−10] Since immobilized domains in thickened UP are not destroyed completely by heating to 120 °C, it is concluded that the main mechanism involved in the viscosity increase is determined by strong electrostatic interactions between Mg^{2+} ions and charged carboxylato chain ends. It appears that the thickening of UP with metal oxides can be described by a mechanism similar to that of ionomers.

Several models have been proposed to explain the morphology of ionomers.[7−10] These models are usually referred to as two kinds of ionic aggregates, designated as multiplets and clusters. On the basis of steric considerations, multiplets are supposed to contain a relatively small number of ionic pairs and consist of ionic material only, whereas clusters are large structures that are rich in ion pairs and contain a considerable quantity of an organic material. The aggregates reveal at least some properties of a separate phase, including a relaxation behavior associated with a higher T_g compared to the T_g of the matrix. It is often suggested that electrostatic interactions play a major role in multiplet formation and aggregation. The elastic nature of the polymer chains opposes aggregation.

The present NMR, WAXD, and SAXS data not only support a mechanism analogous to that in ionomers for the physical gelation of UP but also reveal further details on the molecular structures and phenomena involved. Rheology and conductivity, studied in parallel and to be published separately, show phenomena fully in line with the present investigation.[21] The fraction of the immobilized domains, as determined by ^{1}H NMR T_2-relaxation experiments, represents the proton fraction of immobilized organic material with respect to the total proton content in UP. ^{13}C NMR spectra reveal that only a very small fraction of the styrene protons show significantly reduced mobility, indicating that almost no styrene has been trapped in the immobilized domains. UP1 contains about 50/50 at. % protons of polyester and styrene. Since the immobilized domains are mainly composed of polyester chains, which follows from the ^{13}C NMR data and these domains include more than 30% of the total hydrogen 2 months after the compound was prepared (see Figure 6), these data mean that more than half of the polyester chain units have been incorporated into the immobilized domains after prolonged thickening at 30 °C. On the other hand, the fraction of polyester chain units with high mobility (% T_2^l) is very low, which means that a large part of the remaining UP-chain units experience a reduced mobility and are likewise integrated into the network chains. The fraction of protons with higher mobility, about 20−25% of the total, is much less than the total content of styrene protons. This suggests that about half of the styrene molecules are located in zones with significantly

Table 2. Dependence of % T_2^s, % T_2^{in}, and % T_2^l on the Square Root of the Thickening Time, as Determined by the Slope (in %) and Intercept (in %/h$^{1/2}$), Where Values of % T_2^{in} and % T_2^l for Initial UP Are Given for Comparison

	% T_2^s		% T_2^{in}		% T_2^l	
compound	intercept	slope	intercept	slope	intercept	slope
initial UP0			16		84	
UP1 (20 °C)	2.0	0.56	33.9	0.38	64.0	−0.93
UP1 (30 °C)	1.0	0.77	23.6	1.42	75.7	−2.22
UP3 (30 °C)	1.1	0.52	23.0	1.04	75.7	−1.55

Table 3. Relaxation Parameters at the Thickening Time of 225 h

compound	T_2^s, ms	T_2^{in}, ms	T_2^l, ms	% T_2^s	% T_2^{in}	% T_2^l
initial UP0		2.3	29		16	84
UP1 (20 °C)	0.04	1.0	27	10	40	50
UP1 (30 °C)	0.04	1.0	27	13	45	42
UP3 (30 °C)	0.05	1.4	33	9	39	52

reduced mobility outside the immobilized domains, and the mobility of these styrene molecules is strongly coupled to that of the UP network chains.

According to the ^{13}C NMR data, the mobility of chain units containing unsaturated, carbonyl and ester carbons is hindered in mobility to about the same extent. This suggests that besides electrostatic interactions of Mg^{2+} with carboxylato chain ends several other factors contribute to chain immobilization. These factors could be the following:

(a) Because of the relatively large statistical segment of the polyester chain (about 4−5 rotatable backbone bonds), the anchoring of polyester chain units to immobilized domains causes a restriction in the mobility of a few chain units adjacent to the anchoring site. The immobilized chain portions may also hinder mobility of other polyester chains because of chain entanglements and intermolecular coupling in mobility.

(b) Mg^{2+} ions in salts generally have six coordination sites. The COO^- and/or basic OH^- anions generally occupy four coordination sites of magnesium ions, forming carboxylato and carboxylato-hydroxyl complexes.[18] The remaining two coordination sites are available for other oxygen donor groups, such as the oxygen of a carbonyl group.[50] It has been established that the donor strength with respect to Mg^{2+} decreases in the following line: COO^- > water > glycolic OH > polyester terminal OH > oxygen of ester carbonyl.[16] Terminal OH groups and oxygen of ester carbonyl of UP chains could also form coordination bonds with Mg^{2+} ions which can cause additional chain immobilization.

(c) Ion−dipole interactions between Mg^{2+} ions and dipolar groups of the polyester might also contribute to chain immobilization by Mg^{2+} ions.

The fraction of immobilized domains increases linearly with the square root of the thickening time, as can be seen in Figure 6. This suggests that molecular diffusion is the rate-limiting step in domain formation. This suggestion is supported by the results of the experiment performed for UP1, where thickening was studied at two different temperatures (see Tables 2 and 3), and the results of rheological and dielectric measurements.[21] These methods reveal that the thickening rate increases significantly upon heating which is apparently caused by faster molecular diffusion.

Heating of thickened UP1 causes the following changes. The fraction of immobilized domains, as represented by the fraction of immobilized protons (% T_2^s), decreases upon heating by a factor of about 2−3 (see Figure 10), whereas the mobility of chain units in the domains, as determined by T_2^s, is hardly affected by heating (see Figure 9). It might be suggested that the thickness of the immobilized layer decreases upon heating or that immobilized domains are partially broken down into smaller parts. Strong ionic bonds prevent multiplets from breaking completely even at 120 °C. The following results support this assumption. *First*, the mean molar mass of the network chains, as derived from the T_2^{in} above 80 °C, is close to the molar mass of UP chains. This means that the physical network that is formed by multiplets and chain bridges interconnecting neighboring multiplets remains present at these temperatures. This can only be explained with strong, likewise ionic bonds between carboxylato chain-ends and Mg^{2+}. *Second*, the anchoring of chain ends to multiplets will result in the immobilization of about 3−5 rotatable backbone bonds next to the chain end. The fraction of carboxylato terminated chain-end blocks of this length equals 5−10% of the polyester chain. This value is in the same range as the content of immobilized domains above 50 °C. Above this temperature no further decrease in the domain content upon heating is observed. Upon cooling, the cluster content recovers quickly to a value that is somewhat larger than that before the sample heating (see Figure 10, open point). It suggests that multiplets, which are linked together by bridging chains, are kinetically frozen in the UP matrix even at 120 °C, as a result of which the sample morphology is preserved and the cluster fraction recovers fast upon cooling. It appears that these multiplets act as nucleation centers for fast recovery of the physical structures formed during thickening.

Both NMR and X-ray diffraction provide additional information about the shape of the domains and the morphology. The results of the WAXD, the SAXS, and the spin-diffusion experiments suggest a lamella-like structure of the immobilized domains. According to SAXS and spin-diffusion experiments, the thickness of the immobilized domains hardly changes upon thickening. On the other hand, the proton fraction in immobilized domains increases from a few percent to more than 30%. These results can only be explained if it is assumed that lamella-like structures of about the same thickness grow in lateral direction with increasing thickening time. Lamella-like structures are favored since the ions are situated at UP chain ends, which means that the growth of aggregates in the lateral direction is sterically hindered to a lesser extent than growth in the transverse direction (leading to an increase in their thickness). According to theoretical and experimental studies,[51−58] the average number of dipoles in multiplets for telechelics is 8 times larger than for random ionomers. It should be mentioned in this respect that disklike and lamella-like structures have been observed for ionomers and model compounds which form ionic clusters.[18,59−62]

The thickness of immobilized lamellae as estimated from the spin-diffusion experiment is about 6 nm. This value is larger than the thickness of the crystalline core of the lamellae, which is about 1 nm, as measured by SAXS. This means that a layer of immobilized disordered UP chain units covers the surface of the crystalline lamella and UP chains stick out of the lamella plane (Figure 17a). The thickness of this surface layer is about 2−3 nm according to NMR. The interlamellar distance

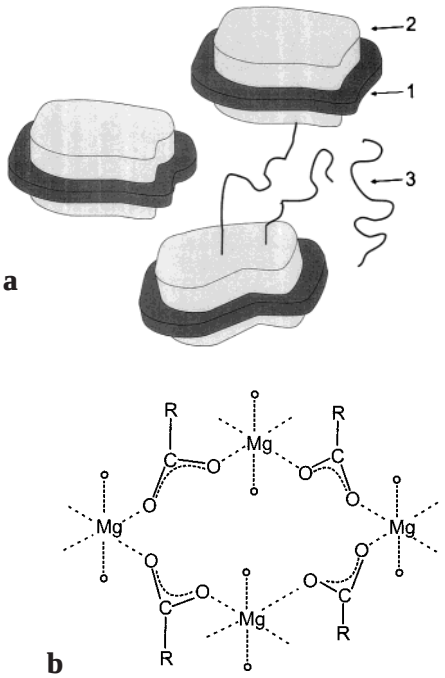

Figure 17. (a) Schematic drawing of the morphology of UP at an intermediate stage of thickening: (1) ion-containing core; (2) immobilized UP phase; (3) phase with network chains, dangling chains, free chains, and styrene. (b) Hypothetical structure of the crystalline core of the lamellae, where open circles represent water molecules. In this figure, just one-fourth of the unit cell is given, corresponding to the asymmetric unit.

is 2−12 nm with a preferred spacing of 3 nm that is comparable to the mean end-to-end distance of UP chains. It is therefore suggested that bridging UP chains at anionic chain ends interconnect the lamellae. In the well-thickened compound, the major fraction of UP chains forms bridges. This follows from the values of % T_2^{in} (see Figures 4 and 6) and the fraction of polyester protons in the compound (about 50 at. %). The schematic drawing of the morphology of thickened UP is shown in Figure 17a.

Molecular Structure of Ionomeric Clusters. Current WAXD data do not provide information on the crystal lattice which is formed by the multiplets. A hypothesis for a more detailed picture is presented here. It is based on the coordination chemistry of Mg−carboxylato complexes. On the basis of the available information from crystal structures, Mg^{2+} ions appear to have a strong preference for coordination to oxygen donor bonds, in particular to water and carboxylato groups. Moreover, the so-called Mg^{2+} carboxylato−aqua complexes are confined to rather strict coordination rules. Mg^{2+} centers prefer an octahedral six-*co*-ordination to oxygen atoms. This primary coordination sphere is preferentially composed of water molecules, but if these are not sufficiently available, the coordination is completed by additional interactions via carboxylato groups. In the secondary coordination sphere hydrogen bonds between water, hydroxyl, and carboxylato groups can be present. These carboxylato groups often form bridging structures involving the coordination of the two oxygen atoms to two different Mg^{2+} centers.[63,64] Chelation, i.e., coordination of the two oxygen atoms of the same group single metal center, has never been observed for Mg^{2+} carboxylates.[65] The interactions via bridging carboxylato groups and hydrogen bonded water molecules often result in 3-dimensional sructures.[66−68] When the carboxylato substituents cause steric hindrances for such 3-dimensional structures, e.g., when the carboxylato groups contain longer chains or bulky groups, a planar structure with an extended Mg^{2+} carboxylato bridge structure is formed.[69] The long organic chains stick out of the plane, closely packed, parallel to each other and perpendicular to the plane. An example of such a crystalline material is bis(phenoxyacetato)bis(aqua)magnesium.[69] The metal ion in this compound is surrounded by two water molecules and four bridging carboxylato groups. These four carboxylato groups are shared with four other metal ions.[69]

It is now hypothesized that lamella-like ionic clusters of a similar structure occur in the MgO-thickened UP. *We can conclude that lamella-like immobilized domains have the following structure.* ***The core part of a lamella is assumed to consist of multiplets which form a planar crystalline lattice composed of Mg^{2+} ions, carboxylato anions at UP chain ends, and the necessary amount of hydroxyl end groups of UP and water molecules to complete the coordination around the Mg^{2+} ions*** *(see Figure 17b).* ***The UP polyester chains stick out of the planar crystal lattice and cover the lateral lamella surface.*** *Growth of the planar structure will be possible by the approach of new Mg^{2+} carboxylato ionic pairs, or of multiplets of such ionic species, toward the side of the planar structure.* ***Chain anchoring to the lamella surface and alignment of chains in the direction perpendicular to the lamella surface cause strong immobilization of chain units adjacent to the lamella surface.*** *UP chains bearing carboxylato group at both chain ends can form bridges with neighboring lamella resulting in the formation of a three-dimensional network.* It is not to be excluded that coordination bonds of hydroxyl end groups of UP chains with Mg^{2+} ions might be another source of bridging chains.

Rheological and Dielectric Data as a Function of Thickening Time. To establish the relationships between molecular processes that accompany the thickening and the macroscopic properties, the results of rheology and dielectric spectroscopy (DIES) for different portions of the same samples are briefly reviewed below. According to the rheological data, thickening of UP by MgO causes systematic changes in the viscoelastic properties with three regions recognizable in the development of the viscosity and phase angle (Figures 1 and 2).

In the first region, which occurs during the first few hours after preparing the compound, an increase in the viscosity is relatively small compared with the final viscosity level. The material behaves like a fluid; i.e., the phase angle equals 90° at 1 Hz. Thus, salt formation does not increase viscosity to the extent suggested by the polymerization mechanism. The conductivity increases only slightly during the first 10−20 h of thickening when MgO is dissolved due to the reaction with carboxylic chain ends.[21]

In the second region, the viscosity increases rapidly, the compound changes from tacky to nontacky material, and the viscous behavior of the compound changes into an elastic one.[21] At the beginning of this stage, the loss modulus is much higher than the storage modulus. The

phase angle drops a little to 85° and stays at the same level for about 2−3 days while the viscosity increases linearly in time. The electrical conductivity, as measured by DIES,[21] decreases by about 1 decade during the second stage, which is apparently caused by an increase in the amount of ionic clusters. This is in line with NMR data, which reveal an increase in the fraction of immobilized domains.

In the third region, the compound does not show a significant change in viscosity. The phase angle drops further during this stage and the viscosity still increases, but it tends to reach a plateau value.[21] After 3 weeks the phase angle approaches a plateau value of about 30°, indicative of extensive viscoelastic behavior.

During the second and third stages the loss peak of the α-relaxation, as measured by DIES,[21] shifts to somewhat higher temperatures (from −45 to −40 °C) and becomes broader while the relaxation strength remains constant. This indicates that polyester chains are increasingly hindered in their mobility and the system becomes more heterogeneous. An increase in T_g, as measured by DIES,[21] occurs more or less simultaneously with the decrease in conductivity. It should be emphasized that the onset of the decrease in conductivity exactly coincides with the appearance of the second transition in the loss index at higher temperatures, indicating the formation of a heterogeneous structure. The strength of dielectric relaxation, which is a measure of the total number of dipoles, does not change significantly during thickening. This suggests that the mobility of the whole UP chain appear to be hindered. A similar conclusion follows from ^{13}C NMR data.

The Molecular Mechanism with Respect to the Viscosity. The following molecular phenomena occur with increasing thickening time.

The first region: The carboxylic acid end groups of UP react with magnesium oxide, which results in the formation of basic and neutral salts. Because of strong electrostatic interactions, "flower"-like micelles with multiplets of Mg^{2+}−carboxylate complexes in the core part and UP chains in the outer parts are formed. Isolated micelles contact each other via the outer parts of their coronas, but bridging chains do not connect them. The viscosity does not change significantly during this stage, because no percolating network is formed by bridging chains.

The second region: Electrostatic interactions between multiplets favor their agglomeration, causing phase separated lamella-like crystalline domains to be formed. Elastic forces of UP chains oppose the agglomeration of multiplets. A continuous network, with bridging chains that interconnect crystalline domains, is formed during this stage. These domains act as multifunctional network junctions. The size of the multiplets could also increase in the second region, since larger multiplets are favorable in telechelics.[51] The increase in the number of network chains and in the fraction of immobilized domains causes a large increase in the viscosity and the storage modulus, and a decrease in conductivity and phase angle. The amount of the domains and the fraction of UP network chains increase linearly with the square root of the thickening time. This suggests that *the limiting factor for these changes is molecular diffusion of polyester chains*. At the end of the second step, the major fraction of polyester chains is incorporated in lamella-like domains and the physical network. This causes the thickening rate to slow down.

The third region: the aggregation of multiplets continues during the third stage, which causes a continuous growth of the immobilized domains at the expense of the mobile network chains. More than half of the polyester chains are built into the immobilized domains two months after the compound was prepared and stored at 30 °C. The remaining chain portions form bridges between neighboring domains. Apparently, the moderate increase in the content of the domains does not result in a significant increase in viscosity. The immobilized domains reveal the second transition in the loss index at higher temperatures.[21] It should be mentioned here that a second T_g can be observed if the domain size has minimum dimensions of 5−10 nm, depending on the technique used to detect the T_g.

Major Factors Affecting the Thickening. According to the results of the present study, the thickening of unsaturated polyesters with MgO can be described by a multiplet-cluster model as was proposed for ionomers by Eisenberg et al.[10] The effect of different factors that affect the physical properties of telechelic ionomers has been studied extensively.[1−10,51−53,57] A short discussion of these factors is provided below.

Temperature. Temperature can have two effects. On one hand, it favors molecular motion, and therefore would tend to increase the rate of the molecular diffusion that is the limiting stage for cluster and network formation. However, an increase in temperature effectively decreases the importance of the Coulombic interactions between the ions and therewith also the importance of the driving force for cluster formation. In this study, we have seen that the thickening rate increases with increasing temperature from 20 to 30 °C (see Tables 2 and 3).

Moisture. From industrial practice, it is known that water helps to accelerate the thickening of UP but lowers the final thickening. It can be assumed that a small quantity of added water, as in the case of UP3, would be uniformly distributed throughout the polyester. After addition of MgO, it is likely that some water molecules, which are adsorbed by MgO and which are furthermore formed during the reaction of MgO with carboxylic end groups, concentrate in the vicinity of the ionic groups. If water solvates the Mg^{2+} ions, some of the carboxylato groups will not form coordination bonds with the Mg^{2+} ions. This reduces the number of UP chains connected to immobilized domains, which is indeed observed by NMR for UP3 (see Tables 2 and 3). This also leads to a decrease in viscosity.[21] It should be mentioned that partial solvatation of MgO with water might accelerate the reaction of MgO with carboxylic chain ends which takes place during the first day after the compound is prepared.

Finally, several chemical characteristics of UP, such as the number of carboxylic groups, the molar mass, and the molar mass distribution of UP molecules, should have a significant effect on the thickening process, since these characteristics apparently determine the number of viscoelastic chains per unit volume and the content, size and shape of multiplets and clusters. A small difference in ionic content between chains can be enough to induce a trend toward phase demixing, since ionic groups strongly interact with one another. This could be a topic for further investigations.

Conclusions

The molecular mechanisms of the thickening of styrene solutions of UP with magnesium oxide have

been studied by solid state NMR, SAXS, and WAXD. It has been shown that the thickening can be described by a mechanism that was proposed for ionomers. The time dependency of the mechanical and dielectric properties, which were simultaneously studied for different portions of the same samples, can be explained by the formation of immobilized domains composed of lamella-like crystalline carboxylato Mg^{2+} aqua complexes in the core part and immobilized polymer chains that stick out of the lamella surface. The lamellae act as multifunctional physical cross-links. On the basis of the established thickening mechanism the influence of different factors on the thickening of polyesters with metal oxides can be explained.

Acknowledgment. The authors are pleased to acknowledge the assistance of S. Knauf and M. Rooijmans in sample preparation, W. F. Zoetelief and J. C. J. F. Tacx for providing results of rheological and DIES experiments, and I. Goudswaard for participation in an early phase of this work. A word of gratitude is due to the management of DSM Resins and DSM Research for their permission to publish this work.

References and Notes

(1) MacKnight, W. J.; Earnest, T. R. *J. Polym. Sci. Macromol. Rev.* **1981**, *16*, 41.
(2) Bailey, F. E., Eisenberg, A., Eds. *Columbic Interactions in Macromolecular Systems*; ACS Symposium Series 302; American Chemical Society: Washington, DC, 1986.
(3) Pineri, M., Eisenberg, A., Eds. *Structure and Properties of Ionomers*, NATO ASI Series: Reidel: Dordrecht, The Netherlands, 1987.
(4) Tant, M. R.; Wilkes, G. L. *J. Macromol. Sci. Macromol. Chem. Phys.* **1988**, *C28*, 1.
(5) Mauritz, K. A. *J. Macromol. Sci. Macromol. Chem. Phys.* **1988**, *C28*, 65.
(6) Bazuin, C. G. In *Multiphase Polymers: Blends and Ionomers*; Utracki, L. A., Weiss, R. A., Eds.; ACS Symposium Series 395, American Chemical Society: Washington, DC 1989.
(7) Schlick, S., Ed.; *Ionomers. Characterization, Theory, and Applications*; CRC Press: Boca Raton, FL, 1995.
(8) MacKnight, W. J.; Lundberg, R. D. In *Thermoplastic Elastomers*, 2nd ed.; Holden, G., Legge, N. R., Quirk, R. P., Schroeder, H. E., Eds.; Hanser Publishers: Munich, Germany, 1996; p 271.
(9) Ikeda, Y. *Int. Polym. Sci. Technol.* **1996**, *23*, T/18.
(10) Eisenberg, A.; Kim, J.-S. *Introduction to Ionomers*; John Wiley and Sons: New York, 1998.
(11) Kia, H. G., Ed. *Sheet Molding Compounds. Science and Technology*; Hanser Publishers: Munich, Germany, 1993.
(12) Szilagyi, A.; Izvekov, V.; Vancsó-Szmercsanyi, I. *J. Polym. Sci.: Polym. Chem. Ed.* **1980**, *18*, 2803.
(13) Rao, K. B.; Gandhi, K. S. *J. Polym. Sci.: Polym. Chem. Ed.* **1985**, *23*, 2135.
(14) Judas, D.; Fradet, A.; Marechal, E. *J. Polym. Sci.: Polym. Chem. Ed.* **1984**, *22*, 3309.
(15) Habassi, C.; Brigodiot, M.; Fradet, A. *Makromol. Chem.* **1990**, *191*, 638.
(16) Vancsó, I.; Szilagyi, A.; Izvekov, V. *J. Polym. Sci.: Polym. Chem. Ed.* **1983**, *21*, 1901.
(17) Han, C. D.; Lem, K. W. *J. Appl. Polym. Sci.* **1983**, *28*, 763.
(18) Laleg, M.; Blanchard, F.; Chabert, B.; Pascault, J. P. *J. Eur. Polym. Sci.* **1985**, *21*, 591.
(19) Judas, D.; Fradet, A.; Marechal, E.; *Polym. Bull.* **1986**, *16*, 13.
(20) Tant, M. R.; Wilkes, G. L. *J. Macromol. Sci., Macromol. Chem. Phys.* **1988**, *C28*, 1.
(21) Tacx, J. C. J. F.; Zoetelief, W. F.; van der Ploeg, A. F. J. M. To be published.
(22) Litvinov, V. M.; Steeman, P. A. M. *Macromolecules* **1999**, *32*, 8476.
(23) Tanaka, H.; Nishi, T. *Phys. Rev. B, Condens. Matter* **1986**, *33*, 32.
(24) Zhang, S.; Mehring, M. *Chem. Phys. Lett.* **1989**, *160*, 644.
(25) Kenwright, A. M.; Say, B. J. *Solid State Nuclear Magn. Reson.* **1996**, *7*, 85.
(26) Cory, D. G.; Ritchey, W. M. *Macromolecules* **1989**, *22*, 1611.
(27) Gotlib, Yu. Ya.; Lifshits, M. I.; Shevelev, V. A.; Lishanskii, I. A.; Balanina, I. V. *Polym. Sci. USSR* **1976**, *18*, 2630.
(28) Fry, C. G.; Lind, A. C. *Macromolecules* **1988**, *21*, 1292.
(29) Litvinov, V. M.; Barendswaard, W.; van Duin, M. *Rubber Chem. Technol.* **1998**, *71*, 105 and references therein.
(30) McBrierty, V. J.; Packer, K. J. *Nuclear Magnetic Resonance in Polymers*; Cambridge University Press: Cambridge, England, 1993.
(31) Schmidt-Rohr, K.; Spiess, H. W. *Multidimensional Solid-State NMR and Polymers*; Academic Press: San Diego, CA, 1994.
(32) Mellinger, F.; Wilhelm, M.; Landfester, K.; Spiess, H. W.; Haunschild, A.; Packusch, J. *Acta Polym.* **1998**, *49*, 108.
(33) Mellinger, F.; Wilhelm, M.; Spiess, H. W. *Macromolecules* **1999**, *32*, 4691.
(34) Clauss, J.; Schmidt-Rohr, K.; Spiess, H. W. *Acta Polym.* **1993**, *44*, 1.
(35) Demco, D. E.; Johansson, A.; Tegenfeldt, J. *Solid State Nuclear Magn. Reson.* **1995**, *4*, 13.
(36) Vonk, C. G. *J. Appl. Crystallogr.* **1973**, *6*, 149.
(37) Vonk, C. G. *J. Appl. Crystallogr.* **1971**, *4*, 340.
(38) Porod, G. In *Small-Angle X-ray Scattering*; Glatter, O., Kratky, O., Eds.; Academic Press: San Diego, CA, 1982.
(39) Baltá-Calleja, F. G.; Vonk, C. G. In *X-ray Scattering of Synthetic Polymers (Polymer Science Library, Vol. 8)*; Jenkins, A. D., Ed.; Elsevier: Amsterdam, 1989.
(40) A wide distribution in the molecular mobility of UP can be caused by several factors. (a) The T_2 relaxation for monodisperse oligomers is usually described by a single exponential function.[41−43] Therefore, the two-component relaxation can be caused by a difference in mobility between the polyester chains and the styrene molecules. However, this is not the only reason for the nonexponential relaxation, since the fraction of polyester and styrene protons in the compound equals about 50 at. % hydrogen, which is less than the fraction of the relaxation component with the longer decay time (84%) corresponding to higher molecular mobility. (b) A wide distribution in molecular mobility of polyester chains themselves due to molar mass distribution and a difference in the mobility between the chain ends and the rest of the chain[43−46] could also result in nonexponential relaxation. (c) The carboxylic and hydroxylic chain ends of polyester chains can form hydrogen bonds, which might also cause a difference in mobility between free and hydrogen bonded polyester chains and/or chain segments. (d) Coupling of the mobility of styrene molecules with that of polyester chains could result in a distribution in the correlation time of styrene molecules.
(41) Kimmich, R.; Bachus, R. *Colloid Polym. Sci.* **1982**, *260*, 911.
(42) Cosgrove, T.; Griffiths, P. C.; Hollingshurst, J.; Richards, R. D.; Semlyen, J. A. *Macromolecules* **1992**, *25*, 6761.
(43) Ries, M. E.; Klein, P. G.; Brereton, M. G.; Ward, I. M. *Macromolecules* **1998**, *31*, 4950.
(44) Weber, H. W.; Kimmich, R. *Macromolecules* **1993**, *26*, 2597.
(45) Kimmich, R.; Köpf, M.; Callaghan, P. *J. Polym. Sci., Part B: Polym. Phys.* **1991**, *29*, 1025.
(46) Kulagina, T. P.; Litvinov, V. M.; Summanen, K. T. *J. Polym. Sci., Part B: Polym. Phys.* **1993**, *31*, 241.
(47) Cohen-Addad, J. P. *Prog. NMR Spectrosc.* **1993**, *25*, 1.
(48) Litvinov, V. M. In *Organisilicon Chemistry II. From Molecules to Materials*; Auner, N., Weis, J., Eds.; VCH: Weinheim, Germany, 1996; p 779 and references therein.
(49) Dujourdy, L.; Bazile, J. P.; Cohen-Addad, J. P. *Polym. Int.* **1999**, *48*, 558.
(50) Young, A. M.; Brigault, C.; Heenan, R.; Higgins, J. S.; Peiffer, D. G. *Polymer* **1998**, *39*, 6685.
(51) Lu, X.; Steckle, W. P.; Weiss, R. A. *Macromolecules* **1993**, *26*, 5876.
(52) Nurkova, I. A.; Khokhlov, A. R.; Doi, M. *Macromolecules* **1993**, *26*, 3601.
(53) Williams, C. E.; Russel, T. P.; Jerome, R.; Horrion, J. *Macromolecules* **1986**, *19*, 2877.
(54) Khalatur, P. G.; Khohlov, A. R.; Nyrkova, I.; Semenov, A. N. *Macromol. Theory Simul.* **1996**, *5*, 713.
(55) Khalatur, P. G.; Khohlov, A. R.; Nyrkova, I.; Semenov, A. N. *Macromol. Theory Simul.* **1996**, *5*, 749.
(56) Khalatur, P. G.; Khohlov, A. R. *Macromol. Theory Simul.* **1996**, *5*, 877.
(57) Horrion, J.; Jérôme, R.; Teyssié, Ph.; Marco, C.; Williams, C. E. *Polymer* **1988**, *29*, 1203.
(58) Semenov, A. N.; Joanny, J.-F.; Khokhlov, A. R. *Macromolecules* **1995** *28*, 1066.
(59) Moudden, A.; Levelut, A. M.; Pineri, M. *J. Polym. Sci., Polym. Phys. Ed.* **1977**, *15*, 1707.

(60) Hashimoto, T.; Sakurai, S.; Morimoto, M.; Nomura, S.; Kojiya, S.; Kodaira, T. *Polymer* **1994**, *35*, 2672.
(61) Hilger, C.; Drager, M.; Stadler, R. *Macromolecules* **1992**, *25*, 2498.
(62) Hilger, C.; Stadler, R. *Macromolecules* **1992**, *25*, 6670.
(63) Malard, C.; Pezerat, H.; Herbin, P.; Toledano, P. *Inorg. Chim. Acta* **1982**, *62*, 241.
(64) White, B.; Vancso-Szmercsanyi, I.; Vancso, G. J. *Polym. Bull.* **1992**, *28*, 95.
(65) Carugo, O.; Djinovic, K.; Rizzi, M. *J. Chem. Soc., Dalton Trans.* **1993**, 2127.
(66) Bock, C. W.; Kaufman, A.; Glusker, J. P. *Inorg. Chem.* **1994**, *33*, 419.
(67) Irish, D. E.; Semmler, J.; Taylor, N. J.; Toogood, G. E. *Acta Crystallogr.* **1991**, *47*, 2322.
(68) Smith, G.; O'Reilly, E.; Kennard, C. H. L. *Inorg. Chim. Acta* **1982**, *62*, 241.
(69) Smith, G.; O'Reilly, E.; Kennard, C. H. L. *J. Chem. Soc., Dalton Trans.* **1980**, 2462.

MA001478Q